Clinics in Surgery

Research Article
Published: 14 Apr, 2022

Image-Guided Percutaneous Biopsy and Pathological Diagnosis in Atypical Imaging Features of Tuberculous Spondylitis

*Ming Lu[#], Wei Chen[#], Zixiong Lei, Shuangwu Dai, Changhe Hou, Shaohua Du, Qinglin Jin and Haomiao Li**

Department of Musculoskeletal Oncology, Center for Orthopaedic Surgery, The Third Affiliated Hospital of Southern Medical University, China

[#]*These authors contributed equally to this work*

Abstract

Background: Atypical tuberculous spondylitis is difficult to distinguish from malignancy and other diseases, leading to misdiagnosis and inadequate treatment. The Purpose of this study was to better elucidate image-guided percutaneous biopsy in the diagnosis of atypical imaging features of tuberculous spondylitis.

Methods: We review retrospectively 8 patients with atypical imaging features of tuberculous spondylitis diagnosed by image-guided percutaneous biopsy. Eight patients with diverse clinical symptoms and atypical imaging features of tuberculous spondylitis were diagnosed by image-guided percutaneous biopsy and imprinted cytology and histology, then, treated by anti-tuberculous medication with or without operation. The incidence of complications (intra- and postoperative), changes in neurological status at final follow-up, and clinical outcomes were evaluated. The neurologic function was evaluated according to the Frankel grading system. Clinical outcomes of the patients were evaluated by Visual Analogic Scale (VAS) scores for pain, imaging (X-ray, CT and MRI) and laboratory examination.

Result: All the eight patients were diagnosed as tuberculous spondylitis by histological and cytological examination of specimens. All of them had anti-tuberculous medication treatment and six of them received operation. One patient suffered pleural effusion after debridement of the thoracic lesion. The mean follow-up period was 16.2 months (6 to 37 months). Decreased VAS scores and improved neurological function were observed in all patients. Solid fusion and osteogenic osteosclerosis were observed at the final follow-up and no recurrences were observed in all cases.

Conclusion: Image guided biopsy and pathological analysis is helpful for early diagnosis of the atypical imaging features of tuberculous spondylitis.

Keywords: Tuberculosis; Spinal infection; Image-guided percutaneous biopsy; Tuberculous spondylitis

OPEN ACCESS

Correspondence:
Haomiao Li, Department of Musculoskeletal Oncology, Center for Orthopaedic Surgery, The Third Affiliated Hospital of Southern Medical University, No.183, Zhongshan Avenue, Tianhe Distract, Guangzhou, 510630, China,
E-mail: lihaomiao1977@hotmail.com

Received Date: *17 Feb 2022*
Accepted Date: *06 Apr 2022*
Published Date: *14 Apr 2022*

Citation:
Lu M, Chen W, Lei Z, Dai S, Hou C, Du S, et al. Image-Guided Percutaneous Biopsy and Pathological Diagnosis in Atypical Imaging Features of Tuberculous Spondylitis. Clin Surg. 2022; 7: 3484.

Introduction

Tuberculosis (TB) was known caused by *Mycobacterium tuberculosis* which was susceptible to older people and immune-compromised patients [1]. Spine is the most common site of musculoskeletal tuberculosis. Tuberculous spondylitis was originally named as 'Pott's Disease', which represents the most common form of extrapulmonary TB [2-4]. The typical imaging manifestations of the spinal tuberculosis are destruction caused by the spread of infection originating from the intervertebral space to the opposing end plates and two adjacent vertebral bodies, with or without a paravertebral abscess [5]. Atypical spinal tuberculosis without the typical features mentioned above is hard to be recognized and diagnosed [6]. The atypical imaging manifestations and the wide range of clinical presentations usually results in difficulties and delay in diagnosis. The degenerative disk disease, pyogenic and fungal infections, inflammatory and neoplastic lesions should be considered as differential diagnosis with the atypical spinal TB [1-3]. Image-guided percutaneous biopsies play an important role in the diagnosis of musculoskeletal lesions. Its accuracy, safety, and cost-effectiveness have been well documented [4]. Here we retrospectively reported a group of atypical imaging features of tuberculous spondylitis diagnosed by image-guided percutaneous biopsy and

pathological analysis. The purpose of this essay was to better elucidate image-guided percutaneous biopsy in the diagnosis of atypical imaging features of tuberculous spondylitis.

Materials and Methods

Patients who were histologically proven tuberculous spondylitis, presenting as atypical imaging features of tuberculous spondylitis in our institution between 2013 and 2020 were retrospectively reviewed from databases and follow-up results. Inclusion criteria of atypical imaging features of spinal tuberculosis are anterior subperiosteal lesion, central form of bony lesion with preserved disc, multi-vertebral lesions (skip lesions), isolated involvement of the posterior elements of the vertebral, extradural mass lesion and intramedullary tuberculoma [3,6-9]. Eight patients (2 females and 6 males) with a mean age of 41.6 years (range, 18 to 61 years) who met these criteria were enrolled. Their clinical presentations, physical examinations, imaging and histopathology studies, laboratory tests, managements, and results of each patient were reviewed. Radiograph, Computerized Tomography (CT), and Magnetic Resonance Imaging (MRI) of the spine were reviewed for each patient. Routine laboratory tests including blood routine, Erythrocyte Sedimentation Rate (ESR), C-Reactive Protein (CRP), Purified Protein Derivative (PPD) test, Tuberculosis Antibody (TA), renal and liver function were performed in all patients. Due to technical limitations, the serum T-SPOT test was only performed in cases after 2016 in our hospital. A decreased ESR and CRP was considered a useful measure of valid response to the treatment. Renal and liver functions were monitored dynamically to detect the hepatorenal toxicity when the patient was taking an anti-tuberculous medication treatment. Biopsy was performed under image-guided by CT or C-arm radiation. The puncture approach and route were based on the location and extent of the lesion. If there are multiple lesions, we tried to puncture from the viable and safe part of the lesions to obtain the specimens. Under the imaging guiding, a 12-gauge core needle biopsy set (Guanlong, Shandong, China) was used to perform the biopsy. After confirming the needle tip had reached the lesion, a specimen was obtained and the needle was withdrawn. The specimens obtained from the biopsy were submitted for cytologic, histologic, and bacteriologic studies. The diagnosis of tuberculous spondylitis was confirmed when histological and cytological examination of specimens reveling granulomas, multinucleated giant cells, Langhan's giant cells or Zeihl-Neelsen stain demonstrating Acid Fast Bacilli (AFB). Operation was performed when considering never compressed with progressive neurological symptoms or vertebral body collapse with deformity or instability. Patients were operated under general anesthesia in a prone position. After exposing the lamina, facet joints and transverse processes from the posterior midline approach, transpedicular screws were installed in the thoracolumbar vertebral body at least one level above and one below the diseased vertebrae. A temporary rod was fixed to stabilize the spine and avoid spinal cord injury during decompression and debridement. Then, a unilateral facetectomy and a semi-laminectomy decompression was performed in the affected side. After pediculectomy in the affected vertebrae, curettage the lesion in the vertebral body was performed through transpedicular approach. The cavity formed after debridement of the lesion inside the vertebral body were filled with autogenous bone from the healthy lamina or autogenous iliac bone graft, and correction of the deformity was accomplished by installing permanent rods with moderate compression maneuvers. Debridement and decompression without fixation were performed in patients who had severe neurological defects or progressive neurological symptoms, with slight bone destruction and good spinal stability. The incidence of complications (intra- and postoperative), changes in neurological status at the final follow-up, and clinical outcomes were evaluated. The neurologic function was evaluated according to the Frankel grading system. Clinical outcomes of the patients were evaluated by Visual Analogic Scale (VAS) scores for pain, imaging (X-ray, CT and MRI) and laboratory examination.

Results

In this series of eight cases (Table 1), all of them presented with atypical imaging features of spinal tuberculosis: One bone lesion in a single lumbar vertebral body with preserved disc; one single thoracic vertebral body lesion with multiple extraspinal bone lesions and six multi-vertebral lesions. All patients presented with back pain and tenderness. Two of them had unexplained recurrent fever. One patient had mild kyphosis deformity in the thoracolumbar junction. Six of them had neurologic deficits on physical and neurological examinations. PPD tests were negative in all the eight patients. Tuberculosis antibody tests were positive in 2 cases. T-SPOT test was performed in 2 cases with both negative results. All eight patients were confirmed the diagnosis of tuberculosis by histological and cytological examination of specimens obtained by image-guided biopsy, which reveling granulomas, multinucleated giant cells, Langhan's giant cells or Zeihl-Neelsen stain demonstrating Acid Fast Bacilli (AFB). All patients received anti-tuberculous medication treatment totally for one year. Two patients who had no neurological deficit symptoms only received antituberculous medication treatment. Decompression by laminectomy, curettage of the lesions transpedicular, and stabilization of the spine by the posterior approach was performed in five cases. One case received debridement and decompression of the thoracic spine without fixation due to progressive neurological symptoms. This patient suffered pleural effusion after debridement of the thoracic lesion and was cured after thoracic drainage. All patients were followed up for at least 6 months (median, 16.2 months; range, 6 to 37 months). Decreased VAS scores and improved neurological function were observed in all patients. At the final follow-up time, back pain and neurological function had completely resolved in all cases. Solid fusion and osteogenic osteosclerosis were observed at the final follow-up and no recurrences were observed in all cases. No complication was observed during the follow-up period.

Cases illustration

Case 1 presentation and examination: A 41-years-old female suffered with low back pain (VAS=9) and bilateral lower limbs numbness for 2 weeks. The patient had neurologic deficit with power grade 4/5 in bilateral lower limbs and sensation decreased bilaterally (Frankel D).

Imaging findings: MRI imaging showed lobulated lesions in L3 vertebral body and the posterior elements, with an epidural lesion causing slight degree of dural compression. Normal signal intensity was observed in the involved L3/L4 intervertebral disc, dural sac, and cauda equina (Figure 1a, 1d). CT scan imaging showed bony destruction involving the posterior elements of the L3 vertebra (Figure 1c, 1e). All characteristics were consistent with a neoplasm. However, the enhanced MRI scan revealed rim enhancement of the vertebral and paravertebral lesions (Figure 1b), which may suggest the possibility of an infectious process.

Laboratory examination: High Erythrocyte Sedimentation Rate

Table 1: Patient information.

No./Age/ Sex	Clinical features	Laboratory examination	Vertebral level	Extrasoinal involvement	Histopathology	Surgery	Anti-TB medication	Complications	Follow-up (months)	Frankel Score*	Quality of life (VAS)*	Imaging#
1/41/F	Pain, radiculopathy	PPD(-) TA(-)	L3	–	Epithelioid granulomata, AFB (+)	DEB+AUTO+STAB	RMP, EMB, PZA, INH, SM	No	12	D→E	9→0	Solid fusion
2/58/M	Pain, fever	PPD(-) TA(-)	T8	+	Numerous neutrophils, AFB (+)	-	RMP, EMB, PZA, INH, SM	No	6	E→E	8→0	Osteogenic osteosclerosis
3/18/M	Pain, fever, kyphosis deformity, radiculopathy	PPD(-) TA(-)	L1, L3, L5	-	Multinucleated giant cells, AFB (+)	DEB+AUTO+STAB	RMP, EMB, PZA, INH, SM	No	20	D→E	9→0	Solid fusion
4/60/M	Pain, radicilopathy	PPD(-) TA(+)	L2, L3	-	Caseous necrosis granulomas	DEB+AUTO+STAB	RMP, EMB, INH, SM	No	24	D→E	6→0	Solid fusion
5/61/F	Pain	PPD(-) TA(-)	C5, T6, L3	-	Langhan's giant cells, AFB (+)	-	RMP, PZA, INH, SM	No	6	E→E	7→0	Osteogenic osteosclerosis
6/35/M	Pain, radiculopathy	PPD(-) TA(+)	L5, S1	-	Multinucleated giant cells, AFB (+)	DEB+AUTO+STAB	PMP, PZA, INH, SM	No	37	D→E	8→0	Solid fusion
7/22/M	Pain, myelopathy	PPD(-) TA(-) T-spot(-)	T11, T12	+	Multinucleated giant cells	DEB+AUTO+STAB	RMP, PZA, EMB, INH, SM	No	17	C→E	5→0	Solid fusion
8/38/M	Pain, myelopathy	PPD(-) TA(-) T-spot(-)	T3-T5, L2, L5	-	Granulomayous inflammation	DEB	RMP, PZA, EMB, INH	Pleural effusion	6	C→E	6→0	Osteogenic osteosclerosis

Abbreviations: DEB: Debridement; AUTO: Autograft; STAB: Stability; VAS scores: Visual Analgue Scale scores; AFB: Acid fast bacilli; RMP: Rifampicin; EMB: Ethambutol; PZA: Pyrazinamide; SM: Streptomycin; INH: Isoniazid; PPD: purified protein derivative test; TA: tuberculosis antibody
*pretreatment→last follow-up, #at last follow-up

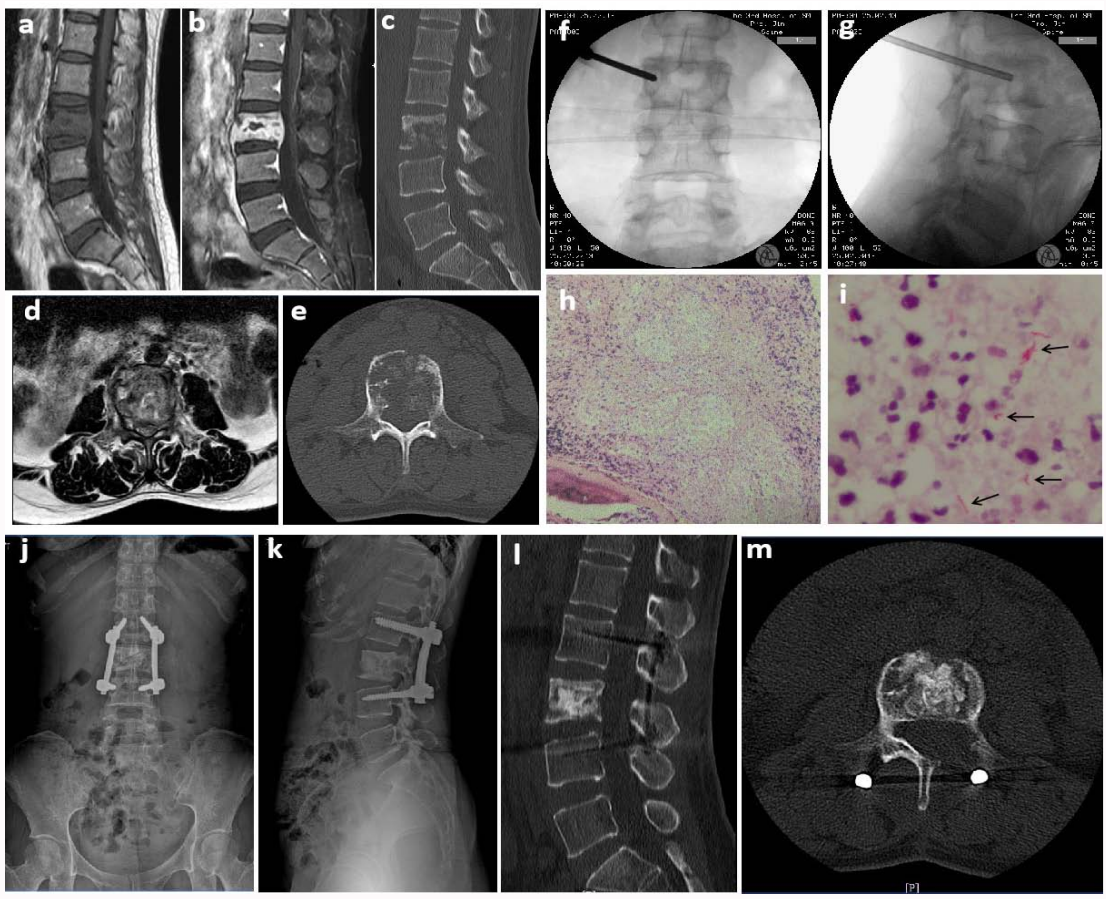

Figure 1: (a, d) Axial and Sagittal MR images showing lobulated pre- and para-vertebral lesion in L3 level with involvement of the L3 vertebral body and the posterior elements, associated with posterior epidural extension through L3 vertebral body, forming epidural lesion causing slight degree of dural compression. (b) Enhanced MRI scan revealed rim enhancement of the L3 vertebral and paravertebral lesions. (c, e) Axial and Sagittal CT images showed bony destruction involving the L3 vertebra. (f, g) Biopsy is performed using a transpedicular approach to obtain L3 vertebral body lesion. (h) The pathologic diagnosis revealed fibro-collagenous tissue with numerous epithelioid granulomata mixed with multinuclear giant cells. (i) Zeihl-Neelsen stain demonstrated acid fast bacilli (AFB) (Arrows). (j, k) Antero-posterior and lateral X-ray images postoperative. (l, m) Axial and Sagittal CT images showed good fusion of the bone grafts inside the L3 vertebral body one year after surgery.

(ESR) (80 mm/h) and C-reactive protein (25.5 mg/l) were showed by blood investigations. PPD test and tuberculosis antibody were both negative.

Management and results: A C-arm-guided biopsy was performed through a transpedicular approach to obtain L3 vertebral body lesions under the prone position (Figure 1f, 1g). The final imprint cytology and histology were performed in the cytopathology laboratory, which revealed fibro-collagenous tissue with numerous epithelioid granulomata mixed with multinuclear giant cells (Figure 1h). Zeihl-Neelsen stain demonstrated Acid Fast Bacilli (AFB) (Figure 1i). These results suggest a diagnosis of tuberculosis. Due to the progressive neurological symptoms, surgery was performed by semi-laminectomy decompression, transpedicular curettage of the lesions, and stabilization of the lumbar spine form posterior approach (Figure 1j, 1k). A combination of anti-tuberculous medication was given pre- and post-operative to this patient for a total of 1 year. She was symptom free (VAS=0, Frankel E) at six months postoperative. CT scan showed solid fusion of the bone grafts inside the L3 vertebral body one year after surgery (Figure 1l, 1m).

Case 2 presentation and examination: A 58-years-old female presented with a 13-month history of bone pain, especially in the back and limbs (VAS=8). In the past six months, she had a history of unexplained recurrent fever and night sweats, with body temperature ranging from 37.0°C to 38.5°C. She had a history of cardiac stent implantation surgery because of coronary heart disease one year ago. The patient's vital signs were stable, with normal muscle strength and sensation (Frankel E). Physical examination was remarkable only for multiple lymph nodes enlargement.

Imaging findings: X ray of the limbs showed lytic bone lesions in the right humerus, right radius, and left fibula (Figure 2a, 2b). CT imaging of the chest and thoracic spine showed pleural effusion, osteolysis and erosion of the T8 vertebra (Figure 2c, 2d). No collapse of intervertebral space and no involvement of the soft tissue of the vertebral body were seen on CT imaging. MRI was not allowed because of cardiac stent implantation.

Laboratory examination: Blood investigations showed high Erythrocyte Sedimentation Rate (ESR) (117 mm/h), high C-reactive protein (>160 mg/l), elevated White Blood Cell (WBC) count and increased serum procalcitonin (0.666 ug/L). All characteristics were consistent with infectious disease.

Management and results: Considering the safety and easily available, we performed biopsy under the guidance of CT at the right humerus lesion (Figure 2e). The pathologic study revealed broken bone tissue with numerous neutrophils, with no granulomata was shown. Zeihl-Neelsen stain demonstrated Acid Fast Bacilli (AFB) which suggested the diagnosis of bone tuberculosis (Figure 2f). Then the patient received general anti-tuberculosis chemotherapy. She was put on a combination of anti-tuberculosis medications included: A combination of Rifampicin (RMP) 450 mg/day, Ethambutol (EMB) 750 mg/day, Pyrazinamide (PZA) 750 mg/day, Isoniazid (INH, 300 mg/day) and Streptomycin (SM) 750 mg/day. The treatment was

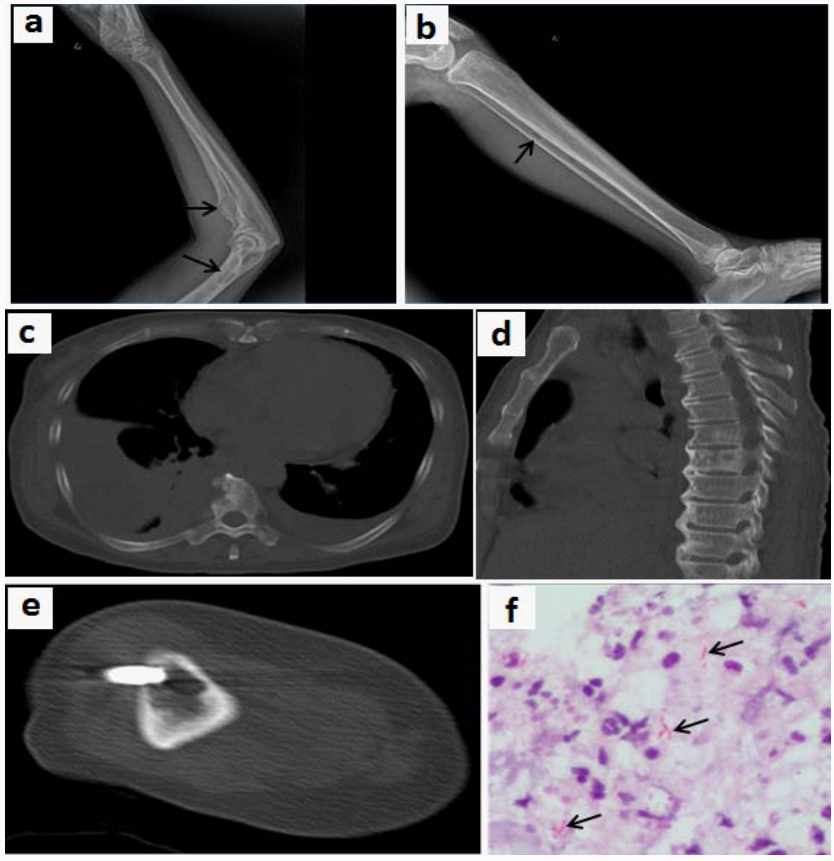

Figure 2: (a, b) X ray of the limbs showed lytic bone lesion in the right humerus, right radius, and left fibula (Arrows). (c, d) CT imaging of the chest and thoracic spine showed pleural effusion, osteolysis and erosion of the T8 vertebra and secondary pathologic fracture. (e) Biopsy is performed using a posterolateral approach on the right humerus lesion. (f) The pathologic diagnosis revealed broken bone tissue with numerous neutrophils without granulomata. Zeihl-Neelsen stain demonstrated Acid Fast Bacilli (AFB) (Arrows).

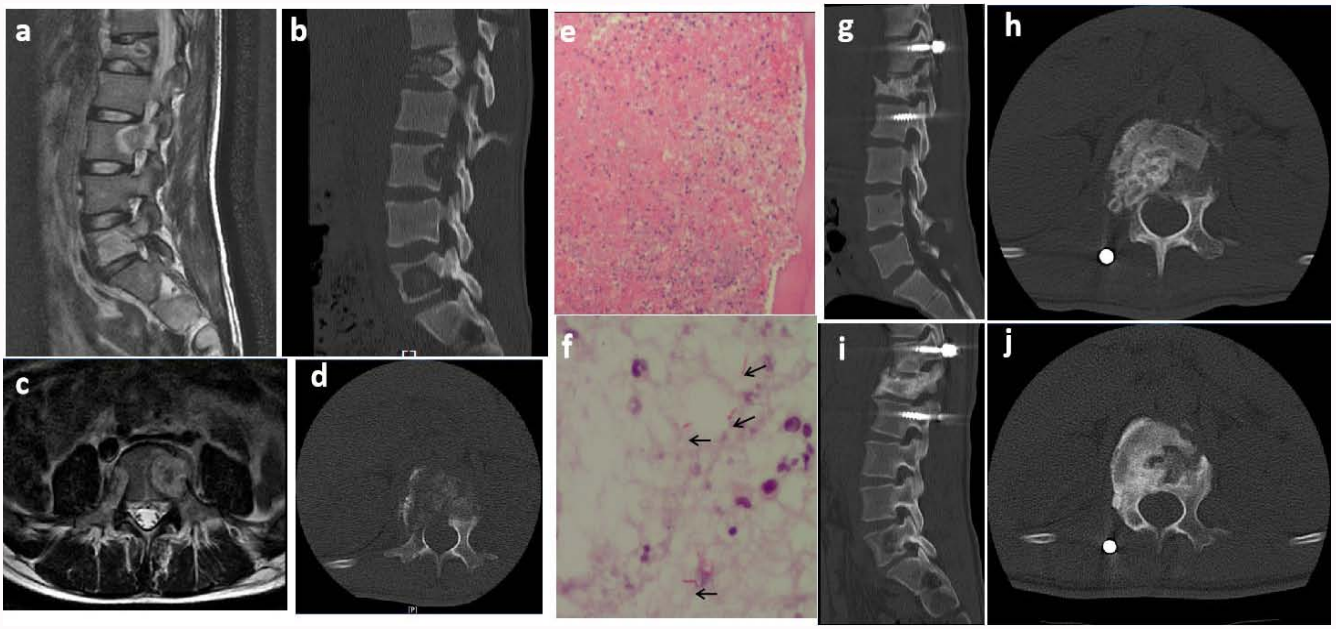

Figure 3: (a, c) Axial and Sagittal MR images showed intrasomatic lytic vertebral lesions in the first and fifth lumbar vertebral body and the third lumbar vertebral pedicle without disk involvement. (b, d) Axial and Sagittal CT images showed Collapse of the L1 vertebral body in addition with dural sac compression. (e) The pathology demonstrated fibro-collagenous tissue with numerous epithelioid cells mixed with multinucleated giant cells. Extensive areas of caseation necrosis were seen. (f) Zeihl-Neelsen stain demonstrated Acid Fast Bacilli (AFB) (Arrows). (g, h) Axial and Sagittal CT images postoperative. (i, j) Axial and Sagittal CT images showed good fusion of the bone grafts inside the L1 vertebral body one year postoperative.

proved effective. After 2 months of medication therapy, she was symptom improved (VAS=4, Frankel E) with no fever and night sweats. Blood investigations showed normal Erythrocyte Sedimentation Rate (ESR) (15 mm/h) and decreased C-reactive protein (14.2 mg/l). Then she was discharged and continued medication (RMP, EBM, PZA, and INH) for another 10 months (total of 1 year). After 6 months of medication therapy, she was symptom free (VAS=0, Frankel E).

Case 3 presentation and examination: An 18-years-old young man presented with a 3-month history of low back pain and unexplained recurrent fever. One week prior to admission, the low back pain was aggravated and he was unable to walk (VAS=8). Physical examination was remarkable for lumbar tenderness, with muscle strength and sensation decreased in bilateral low extremities (Frankel D).

Imaging findings: CT and MRI revealed intrasomatic lytic vertebral lesions in the first and fifth lumbar vertebral body and the third lumbar vertebral pedicle without intervertebral space involvement. Collapse of the L1 vertebral body leading to dural sac compression was observed (Figures 3a-3d).

Laboratory examination: Blood investigations showed high Erythrocyte Sedimentation Rate (ESR) (98 mm/h) and high C-reactive protein (10.68 mg/l). PPD test and tuberculosis antibody were both negative.

Management and results: For this patient, a biopsy was performed using a transpedicular approach to obtain L1 vertebral body lesions under prone position. The pathologic diagnosis revealed fibro-collagenous tissue with numerous epithelioid cells mixed with multinucleated giant cells (Figure 3e). Zeihl-Neelsen stain demonstrated Acid Fast Bacilli (AFB) (Figure 3f). The pathological study was consistent with caseating granulomatous tuberculous. Considering L1 vertebral collapse and mild kyphosis deformity with neurological impairment, transpedicular curettage of the L1 vertebral lesions, with kyphosis deformity correction and stabilization of the spine by posterior approach was performed (Figure 3g, 3h). At six months postoperative, he was symptom free (VAS=0, Frankel E). CT scan showed solid fusion of the L1 vertebral body one year after surgery (Figure 3i, 3j).

Discussion

Spinal tuberculosis is one of the oldest diseases known to mankind with common occurrence and high morbidity and mortality in people with low immunity or poor nutritional status [5]. Early diagnosis and treatment are considered to be the most important strategy to save neurological function and prevent spinal deformity [5]. However, there is no sufficient discussion on the diagnostic and treatment criteria for the atypical spinal tuberculosis. According to the principle "don't biopsy if not to be treated", biopsy is indicated when a lesion requires tissue sampling for determining diagnosis, stage of malignancy, and treatment [5]. In cases of spinal TB, especially in some atypical imaging features of spinal TB which are tricky to diagnose, biopsy is indicated for differential with vertebral neoplasm and pyogenic spondylitis [5]. Compared to incisional biopsy, image-guided percutaneous needle biopsy is much safer with precise location display, easy and quick execution, and it also has a lower risk of complications [10]. Reported percutaneous risk rates are 0 to 10%, whereas a up to 16% for open biopsy was reported by the literature [11,12]. Hemorrhage, nerve injury, and infection are the main complications in percutaneous biopsy [11]. Currently, CT is considered to be the best imaging-guide method for bone biopsy [13]. As it provides the accurate three-dimensional structure of lesion location, which is conducive to better formulation of puncture route that safely avoids neurovascular structure injury [13,14]. Puncture needle biopsy guided by C-arm is a commonly used modality for performing bone biopsy. Compared to CT, it is less ionizing radiation

and cost, with a shorter procedure time. However, its accuracy in targeting lesions is imprecise and poor demonstrating of the soft tissue lesions. Therefore it is usually applied to biopsy of large bone lesions without vital neurovascular structure involvement, which are easy and safe to get specimens. The majority of percutaneous vertebral biopsies are performed through posterior approach. Approach through bone structures (transpedicular) is safer than soft tissue, and it is more effective to biopsy lytic zones than blastic ones. Transpedicular procedure is a correct way to get specimens of the lesion from a vertebral body without violating the epidural space. The perforation must be cautious to avoid breakage of the pedicle with consequent epidural space contamination [15]. When multiple lesions are present, the selection of biopsy site and puncture approach should be comprehensively considered including the safety of access, easily available, and aggressive image observations. Etiological confirmation can be made either by demonstration of acid-fast bacilli on the pathological specimens or histological evidence of a tubercle or the mere presence of epithelioid cells on the biopsy material [16]. Conventional methods like Ziehl-Neelsen staining for acid-fast bacilli and culture of mycobacterium tuberculosis were considered with low sensitivity and specificity [17]. Only a 52% smear positivity rate for acid-fast bacilli was reported by the literature [18]. The cytology sample may help us to confirm the inflammatory process including direct visualization of pathogens. In our case series, acid-fast bacilli were observed under the microscope in 5 cases, which suggested the diagnosis of tuberculosis. Finally, the anti-tuberculosis medication was proven effective in these cases, which further confirmed the diagnosis of tuberculosis. Culture positivity rate of mycobacterium tuberculosis was 83% [18]. However, the culture is time consuming, usually takes 6 to 8 weeks for the growth to appear [19]. Therefore, histological evidence on the diagnosis of tuberculosis is critical. Literature review shows that approximately 60% of the spinal tuberculosis patients were confirmed by histologic studies [5]. Epithelioid cell granulomas, granular necrotic background, and lymphocytic infiltration are the most three common cytological findings observed in histologic studies [20]. While typical scattered multinucleated and Langhans' giant cells were observed in only 56% of patients [20]. A false-negative result of biopsy in tuberculosis is rarely seen. When bacteriology proves negative, a diagnostic treatment by anti-tuberculosis medication can be considered if the clinical symptoms and imaging are insufficient to make a definite diagnosis [5]. The treatment principles for atypical spinal TB are similar to typical cases [21]. Anti-tuberculosis medication treatment was considered essential and should be started as early as possible [5]. The precise role of surgery in the management of spinal tuberculosis is controversy. Literature reported that different degrees of neurological recovery can be observed in approximately 40% of spinal tuberculosis patients with paraplegia who treated with anti-tuberculosis treatment, rest and/or traction [22]. Anti-tuberculous treatment alone can be effective in improving neurological symptoms and preventing the progression of spinal deformity [22,23]. In some cases, however, surgery may be indicated with the benefits including: rapid pain relief, effective neurological recovery, less deformity progression, earlier mobility, higher bone fusion rate, and short hospital time [5]. Some experts suggested that the indications for surgery were tissue sampling when the diagnosis is doubtful, clinical deterioration or lack of clinical improvement, evolving neurological deficit, recurrent neurologic complications, abscess drainage in the cervical spine, large paravertebral abscess drainage, spinal instability, pan-vertebral lesions, severe kyphptic deformity, and refractory disease [24-30]. E. Oguz [27] proposed a new classification used to guide the surgical treatment of spinal tuberculosis, which was based on seven clinical and radiological criteria (abscess formation, disc degeneration, vertebral collapse, kyphosis, sagittal index, instability and neurological problems). This classification system divides tuberculosis of the spine into three types and recommends specific techniques for each type (drug treatment, abscess drainage and debridement, debridement and fusion with/without decompression, debridement and fusion with/without decompression and correction of deformity with internal fixation). We first reported one-stage anterior interbody autografting and instrumentation in thoracolumbar spinal tuberculosis with a remarkable clinical efficacy in 2004 [28]. One-stage posterior debridement through transpedicular approach was adopted in our case followed by anti-tuberculous treatment in this study. Recently, Wang et al. [29] reported that one-stage posterior focus debridement using titanium mesh cages and posterior instrumentation achieved very good clinical results in aged patients with lumbosacral spinal tuberculosis. One stage anterior or posterior approach surgery in selected cases, which greatly improves the efficiency and safety of the operation. These types of surgical approach have been used extensively for the management of spinal TB. It is a viable and safe surgical option for treatment in thoracic or lumbar spinal TB [27]. Appropriate choice of the timing, indication and procedure of surgical intervention is vital to the treatment of spinal tuberculosis. One limitation of this study is the small sample number that only 8 cases were included. Selection bias was conducted including patients with atypical imaging features of tuberculous spondylitis. As mentioned above, the inclusive criteria for this study are limited, so will be the sample size. Further studies with control groups and large sample size are required to establish a definitive role of the image-guided biopsy and pathological analysis in diagnosis of atypical tuberculous spondylitis. Furthermore, due to the limitations in application of the emerging technologies, like the serum T-SPOT test and PCR analysis, the diagnosis and treatment for atypical tuberculous spondylitis are delayed to a certain extent in our study.

Conclusion

In summary, atypical spinal TB has been well documented and is difficult to distinguish from nonspecific infections and malignancies, leading to misdiagnosis and inadequate treatment. If the clinical and imaging findings are insufficient for differential diagnosis, image-guided biopsy and pathological analysis is helpful for early diagnosis.

Funding

This work is financially supported by Research and Development Projects in Key Areas of Guangdong Province (NO. 2019B020201015), and the Natural Science Foundation of Guangdong Province (NO. 2021A1515011313).

References

1. Jevtic V. Vertebral infection. Eur Radiol. 2004;14:E43–E52.
2. Moore SL, Rafii M. Imaging of musculoskeletal and spinal tuberculosis. Radiol Clin North Am. 2001;39(2):329-42.
3. Moorthy S, Prabhu NK. Spectrum of MR imaging findings in spinal tuberculosis. AJR AM J Roentgenol. 2002;179(4):979-83.
4. Le HB, Lee ST, Munk PL. Image-guided musculoskeletal biopsies. Semin Intervent Radiol. 2010;27:191-8.
5. Garg RK, Somvanshi DS. Spinal tuberculosis: A review. J Spinal Cord Med. 2011;34(5):440-54.

6. Khattry N, Thulkar S, Das A, Khan SA, Bakhshi S. Spinal tuberculosis mimicking malignancy: Atypical imaging features. Indian J Pediatr. 2007;74(3):297-8.
7. Thammaroj J, Kitkhuandee A, Sawanyawisuth K, Chowchuan P, Promon K. MRI findings in spinal tuberculosis in an endemic country. J Med Imaging Radiat Oncol. 2014;58(3):267-76.
8. Zhen P, Li XS, Lu H. Single vertebra tuberculosis presenting with solitary localized osteolytic lesion in young adult lumbar spines. Orthop Surg. 2013;5(2):105-11.
9. Yang Y, Wang X, Du B, Yuan W, Ni B, Chen D. Isolated atypical spinal tuberculosis mistaken for neoplasia: Case Report and literature review. Eur Spine J. 2013;22(3):S302-305.
10. Rivas-Garcia A, Sarria-Estrada S, Torrents-Odin C, Casas-Gomila L, Franquet E. Imaging findings of Pott's disease. Eur Spine J 2013;22:567-78.
11. Welker JA, Henshaw RM, Jelinek J, Shmookler BM, Malawer MM. The percutaneous needle biopsy is safe and recommended in the diagnosis of musculoskeletal masses. Cancer. 2000;89:2677-86.
12. Mankin HJ, Mankin CJ, Simon MA. Members of the musculoskeletal tumor society. The hazards of the biopsy, revisited. J Bone Joint Surg Am. 1996;78:656-63.
13. Jain R, Sawhney S, Berry M. Computed tomography of vertebral tuberculosis: Patterns of bone destruction. Clin Radiol. 1993;47:196-9.
14. Peh WCG. CT-guided percutaneous biopsy of spinal lesions. Biomed Imaging Interv J. 2006;2-3:e25.
15. Gasbarrini A, Cappuccio M, Donthineni R, Bandiera S, Boriani S. Management of benign tumors of the mobile spine. Orthop Clin North Am. 2009;40(1):9-19.
16. Skaf GS, Kanafani ZA, Araj GF, Kanj SS. Non-pyogenic infections of the spine. Int J Antimicrob Agents. 2010;36(2):99-105.
17. Kramer N, Rosenstein ED. Rheumatologic manifestations of tuberculosis. Bull Rheum Dis. 1997;46(3):5-8.
18. Francis IM, Das DK, Luthra UK, Sheikh Z, Sheikh M, Bashir M. Value of radiologically guided Fine Needle Aspiration Cytology (FNAC) in the diagnosis of spinal tuberculosis: A study of 29 cases. Cytopathology. 1999;10(6):390-401.
19. Cheng VC, Yam WC, Hung IF, Woo PC, Lau SK, Tang BS, et al. Clinical evaluation of the polymerase chain reaction for the rapid diagnosis of tuberculosis. J Clin Pathol. 2004;57-3:281-5.
20. Jutte PC, Van Loenhout-Rooyackers JH. Routine surgery in addition to chemotherapy for treating spinal tuberculosis. Cochrane Database Syst Rev. 2006;25(5):CD004532.
21. Momjian R, George M. Atypical imaging features of tuberculous spondylitis: Case report with literature review. J Radiol Case Rep. 2014;8(11):1-14.
22. Tuli SM. Results of treatment of spinal tuberculosis by 'middle path' regime. J Bone Joint Surg Br. 1975;57-1:13-23.
23. London: Royal College of Physicians. National Collaborating Centre for Chronic Conditions. TB (partial update) clinical guideline DRAFT (November 2010). Tuberculosis: Clinical diagnosis and management of tuberculosis, and measures for its prevention and control.
24. Jutte PC, Castelein RM. Complications of pedicle screws in lumbar and lumbosacral fusions in 105 consecutive primary operations. Eur Spine J. 2002;11(6):594-8.
25. Sell P. Expert's comment concerning grand rounds case entitled 'Posterior listhesis of a lumbar vertebra in spinal tuberculosis' (by Matthew A. Kirkman and Krishnamurthy Sridhar). Eur Spine J. 2011;20(1):6-8.
26. Jain AK. Tuberculosis of the spine. A fresh look at an old disease. J Bone Joint Surg Br. 2010;92(7):905-13.
27. Oguz E, Sehirlioglu A, Altinmakas M, Ozturk C, Komurcu M, Solakoglu C, et al. A new classification and guide for surgical treatment of spinal tuberculosis. Int Orthop. 2008;32(1):127-33.
28. Jin D, Qu D, Chen J, Zhang H. One-stage anterior interbody autografting and instrumentation in primary surgical management of thoracolumbar spinal tuberculosis. Eur Spine J. 2004;13(2):114-21.
29. Wang YX, Zhang HQ, Liao W, Tang MX, Guo CF, Deng A, et al. One-stage posterior focus debridement, interbody graft using titanium mesh cages, posterior instrumentation and fusion in the surgical treatment of lumbo-sacral spinal tuberculosis in the aged. Int Orthop. 2016;40(6):1117-24.
30. Qian J, Rijiepu A, Zhu B, Tian D, Chen L, Jing J. Outcomes of radical debridement versus no debridement for the treatment of thoracic and lumbar spinal tuberculosis. Int Orthop. 2016;40(10):2081-8.